ADVANCED FUNCTIONAL MATERIALS
www.afm-journal.de

Towards All-Solid-State Polymer Batteries: Going Beyond PEO with Hybrid Concepts

*Yi-Hsuan Chen, Peter Lennartz, Kun Ling Liu, Yi-Chen Hsieh, Felix Scharf, Rayan Guerdelli, Annika Buchheit, Mariano Grünebaum, Fabian Kempe, Martin Winter, and Gunther Brunklaus**

To go beyond polyethylene oxide in lithium metal batteries, a hybrid polymer/oligomer cell design is presented, where an ester oligomer provides high ionic conductivity of 0.2 mS cm^{-1} at 40 °C within thicker composite cathodes with active mass loadings of up to 11 mg cm^{-2} ($LiNbO_3$-coated) $LiNi_{0.6}Mn_{0.2}Co_{0.2}$ (NMC622), while a 30 µm thin scaffold-supported polymer electrolyte affords mechanical stability. Corresponding discharge capacities of the hybrid cells exceed 170 mAh g^{-1} (11 mg cm^{-2}) or 160 mAh g^{-1} (6 mg cm^{-2}) at rates of either 0.1 or 0.25 C. Multilayer pouch cells are projected to enable energy densities of 235 Wh L^{-1} (6 mg cm^{-2}) and even up to 356 Wh L^{-1} (11 mg cm^{-2}), clearly superior to other reported polymer-based cell designs. Polyester electrolytes are environmentally benign and safer compared to common liquid electrolytes, while the straightforward synthesis and affordability of precursors render hybrid polyester electrolytes suitable candidates for future application in solid-state lithium metal batteries.

1. Introduction

The world is currently experiencing energy and environmental challenges that strongly affect daily life and social developments.[1] In the mobility sector, electrical vehicles (EVs) have gained a significant amount of interest due to their potential to reduce environmental impacts of traditional automotive vehicles.[2] In view of attractive features including high energy and power density, straightforward processing, and manufacturing, as well as environmental friendliness, rechargeable battery systems based on lithium-ion batteries (LIBs) or lithium metal batteries (LMBs) are recognized as viable options for contemporary EV applications. In particular, LMBs are considered as candidates for high energy density storage due to their high specific and volumetric capacity compared to commercially well-established LIBs that often utilize graphite-type anodes.[3] An increased amount of exploitable cell capacity necessitates higher safety standards that may be achieved by invoking solid polymer electrolytes that do not contain high vapor pressure constituents like liquid electrolytes.[4] LMBs commercialized by Blue Solutions (part of the Bolloré group) are comprised of lithium metal anodes and lithium iron phosphate (LFP) cathodes in addition to polyethylene oxide (PEO) separator membranes that operate at temperatures between 60 and 80 °C.[5] Though environmentally benign, the LFP cathode active material is limited in performance. The cell voltage (3.5 V during discharge) and the achievable specific capacity (practically ≈160 mAh g^{-1}) are inferior compared to modern cathode active materials such as lithium nickel-manganese-cobalt oxide (NMC). Specifically, $LiNi_{0.6}Mn_{0.2}Co_{0.2}O_2$ (NMC622) affords a discharge voltage of ≈3.7–3.8 V and a practical capacity of ca. 175 mAh g^{-1} (theoretical: 275 mAh g^{-1}), and is thus more suitable to reach higher specific and volumetric energy densities of considered cells.[6]

In an effort to develop superior materials to conventional PEO-type electrolytes, star-shaped polyesters have been introduced: grafted cyclodextrin-polycaprolactone (GCD-PCL, **Figure 1**) and benzene-1,3,5-triol polycaprolactone (Bt-PCL).[7] Grafted polymers on cyclodextrins (GCDs) constitute an alternative and advantageous approach for the rational design of hyper-branched architectures in contrast to rather intricate synthesis of poly-rotaxanes, where the macrocycles are often threaded onto PEO-type matrices.[8] These α-CDs are cyclic oligosaccharides produced from starch and are well-known in the field of food chemistry.[9] When considering aspects of "green chemistry", PCL-grafted CDs can be obtained with a minimum amount of organic solvents when using organic-based catalysts, rendering synthesis relatively environmentally benign. Unlike GCD-PCL, the widely available PEO typically requires

Y.-H. Chen, P. Lennartz, K. L. Liu, Y.-C. Hsieh, F. Scharf, R. Guerdelli, A. Buchheit, M. Grünebaum, F. Kempe, M. Winter, G. Brunklaus
Forschungszentrum Jülich GmbH
Helmholtz Institute Münster
IEK-12, Corrensstraße 46, 48149 Münster, Germany
E-mail: g.brunklaus@fz-juelich.de

M. Winter
MEET Battery Research Center
Institute of Physical Chemistry
University of Münster
Corrensstraße 46, 48149 Münster, Germany

The ORCID identification number(s) for the author(s) of this article can be found under https://doi.org/10.1002/adfm.202300501.

DOI: 10.1002/adfm.202300501

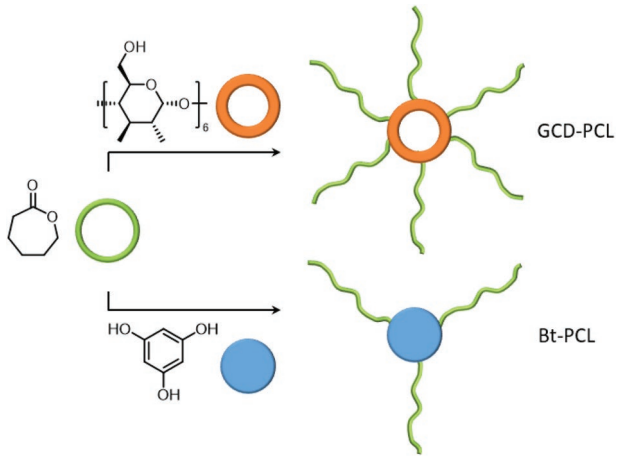

Figure 1. Polymer electrolytes prepared from ε-caprolactone by ring-opening polymerization, yielding a hyper-branched polymer GCD-PCL or previously reported three-arm star polymer Bt-PCL.[7]

the reaction of toxic ethylene oxide (EO) species, unless very refined block copolymer designs are utilized.[10]

Herein, cross-linked poly(caprolactone) based grafted cyclodextrins (xGCD-PCL) are introduced as a novel class of solid polymer electrolytes with electrochemical features that go beyond those of PEO. Based on its weaker coordination of Li^+ ions compared to ether-type polymers, variants of poly(ε-caprolactone) (PCL) may enable faster Li-ion transport and hence conductivity, while their biodegradability is exploited in biomedical applications, such as drug delivery systems or implants for orthopedic surgery.[11] In terms of the electrochemical stability, the relatively low basicity of PCL allows for lower HOMO levels compared to crystalline PEO, resulting in sufficient oxidative stability against high voltage cathode materials.[12] The weaker coordination of ester groups to Li^+ also enables a higher transference number compared to PEO, thereby boosting the battery performance at higher C-rates. However, the charge carrier transport remains limited at temperatures below 40 °C.[13] Numerous attempts of tweaking the polymer architectures toward better battery performance were explored recently, including block copolymers, hybrid materials and hyper-branched polymers, although these studies mainly considered cells at low C-rates and elevated operational temperatures.[14] In addition, network ion solvation structures that may provide scaffolds for 3D charge carrier transport have been proposed.[8c,d,15]

Both, xBt-PCL and xGCD-PCL polymer electrolytes operate at 40 °C, which is close to the operating temperature window of Li-ion batteries.[16] Though both polyesters are improvements compared to PEO based on operating temperature (40 vs 60 °C for PEO), they showed deficiencies in specific capacity and higher internal resistances. Herein a hybrid cell concept and strategy to mitigate these limitations is presented; the cell thickness is reduced by using a thin separator matrix, thereby boosting the energy density. This approach is comparable to thin separator designs made of PEO and PMMA membranes, though these were evaluated in combination with LFP and not NMC-type cathodes.[6b,17]

Furthermore, it is demonstrated here that the specific discharge capacity of the active material can be improved up to >160 mAh g^{-1} by utilizing ester-based oligomers as visco-elastic electrolyte/additive within the composite cathodes. Indeed, ester oligomers are considered beneficial based on their affordability compared to ionic liquids, whose production costs did not decrease as originally forecasted some years ago.[18] A previously reported in situ polymerization of 1,3-dioxolane (DOL) monomers inside the cathode is similar in concept but should be classified as "quasi-solid" electrolyte due to the unfavorably low boiling point (76 °C) of residual DOL monomers.[19] In addition, a hybrid oligomer additive consisting of bismaleimide (BMI) and polyether monoamine (Jeffamine-M1000) moieties was previously exploited as protective coating on particle surfaces of NMC811 and NCA (lithium nickel cobalt aluminum oxide) in a liquid-electrolyte cell system.[20] The introduced key strategy of combining thin matrix-supported separator polymer membranes with firstly reported oligomer catholytes in a hybrid cell set-up allows for higher cathode mass loadings, thereby enabling significantly improved polymer-based LMBs. Polymer/oligomer hybrid electrolytes also exhibit better thermal properties compared to established liquid electrolytes.

2. Results and Discussion

The proposed strategy to go beyond PEO is presented in more detail in the following chapters. After the description of the overall thin-film solid state design, we elaborate the synthesis and characterization of the electrolyte components and continue with the role of oligomers within the cathode. Finally, performance of lab-scale cell prototypes is presented, as well as a discussion of remaining challenges and limitations, as well as achievable benefits in view of projected energy densities of the polymer-based hybrid cells.

2.1. Thin-Film Solid State Design

A hybrid cell concept for polymer-based solid-state batteries is introduced here to enable higher energy densities, as shown in **Scheme 1**a. Previously reported solid-state cells of type "Generation I" were assembled with a 100 µm thick polymer membrane to yield free standing membranes that can be readily processed.[7] By using a matrix-supported separator in which a scaffold contributes to the actual mechanical stability,[17c] ($G' \approx$ 0.2 MPa, Figure S21, Supporting Information), the electrolyte membrane thickness can be reduced to 30 µm (i.e., Generation II). In practice, such thin hybrid membranes are produced based on a 5 µm polyethylene (PE) scaffold, which is placed between two 25 µm polymer membranes and the resulting layered sandwich is hot-pressed into thin solid polymer electrolyte (SPE) membranes with a thickness of 30 µm, as monitored by scanning electron microscopy (SEM, **Figure 2**a–c).

A photograph of the transparent xBt-PCL thin membrane with a diameter of 14 mm is shown in Figure 2d. Notably, a solvent-free approach can be applied to any polymer with a melting point below 100 °C. Three kinds of polymers were transformed into thin hybrid membranes—xBtH, xGCDH, and xPEOH (x stands for cross-linked and H for hybrid). All the PCL-based electrolytes were anticipated to surpass PEO in terms of specific

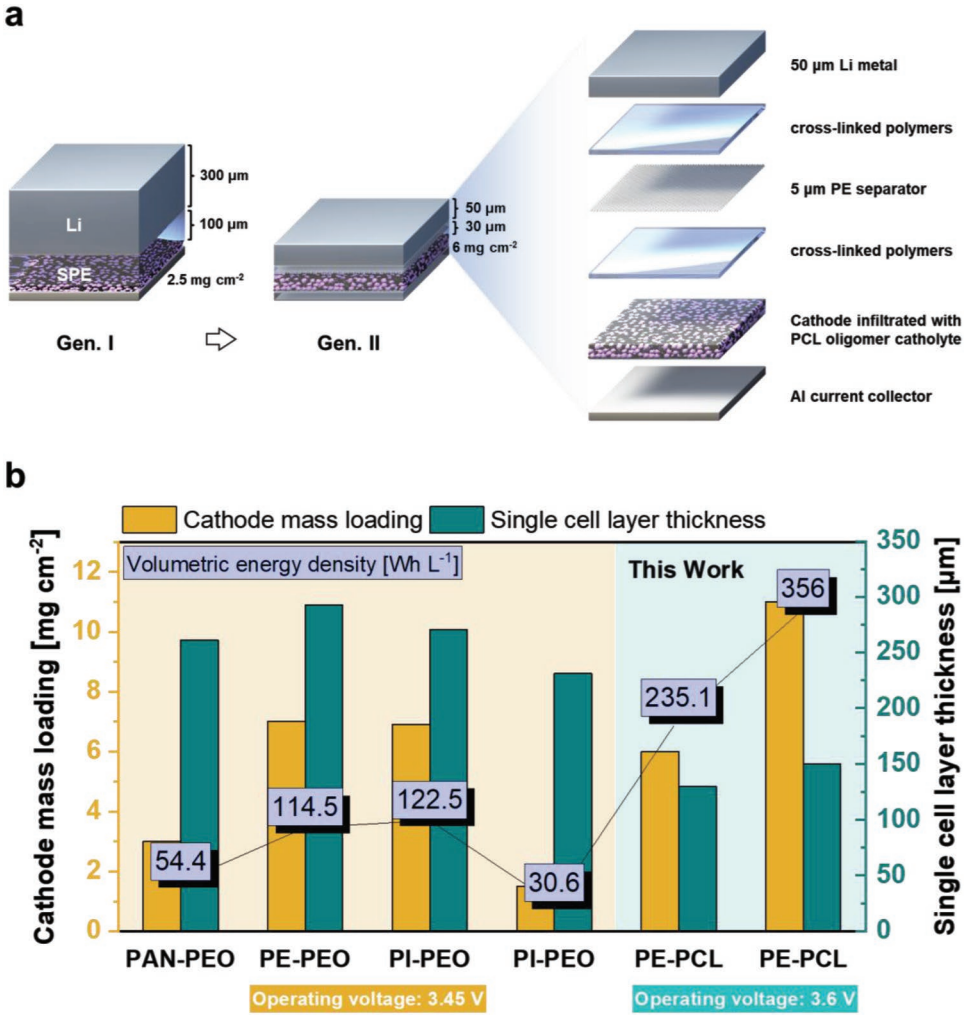

Scheme 1. a) From "Generation I" to "Generation II" polymer-based LMB hybrid cell set-up: thinner lithium metal and solid polymer electrolyte with thicker (high-mass loading) cathodes. b) Comparison of cathode mass loading, cell thickness and volumetric energy density among state-of-the-art thin-film solid polymer batteries. Note that except for our work, the available data reflect cell designs based on LFP-type cathodes with comparable mass loadings of up to 7 mg cm^{-2}. See Table S2 (Supporting Information) for more details (volumetric energy density: projected value from 15-layered pouch cells; the overall single cell layer thickness includes the thickness of the corresponding polymer-based electrolyte, Li metal anode, cathode, and current collector(s), respectively).

capacity and cycling performance, attributing to their higher t^+ values and oxidative stability. A "Generation I" cell set-up was constructed in using an excessive amount (300 µm) of lithium metal electrode compared to merely 2.5 mg cm^{-2} of cathode active material mass loading (0.44 mAh cm^{-2} at a specific capacity of 175 mAh g^{-1}). For "Generation II" cells, 50 µm lithium metal anodes were used and the cathode mass loading was increased to 6 mg cm^{-2} (1.05 mAh cm^{-2}). Initially, the higher mass loading delivered reduced capacities of 34 mAh g^{-1} at 40 °C and rates of 0.2C when operating NMC622|xBt-PCL|Li cells. Caprolactone oligomers (PCL400) were introduced as a catholyte additive, exhibiting ionic conductivities of up to 0.2 mS cm^{-1}, one magnitude higher than xBt-PCL. The 6 mg cm^{-2} cathode was infiltrated with flowable viscoelastic oligomer to boost the lithium-ion transfer within the cathode particles. To obtain a realistic perspective of the achievable energy density, a 15-layered pouch cell was modelled with parameters described in the Supporting Information. Thus, the projected energy density can be enhanced by ≈700 % when going from "Generation I" (30 Wh L^{-1}) to "Generation II" (235 Wh L^{-1}), as summarized in Scheme 1b comparing available data of state-of-the-art thin-film polymer-based batteries, solely operating LFP-based cathodes with comparable mass loadings of up to 7 mg cm^{-2}, in contrast to the introduced cells operating against the higher voltage cathode NMC622 at mass loadings of up to 11 mg cm^{-2}, clearly illustrating the provided advancement of the introduced hybrid cell concept. The resulting overall single cell layer thickness below 150 µm (including the thickness of the corresponding polymer-based electrolyte, Li metal anode, cathode, and current collector(s)) affords a projected superior energy density of 356 Wh L^{-1}, even higher than in case of Bolloré-type PEO-based cells, (also see Table S2, Supporting Information). Notably, a solvent-free approach was proposed for preparing thin hybrid electrolytes, therefore no highly flammable

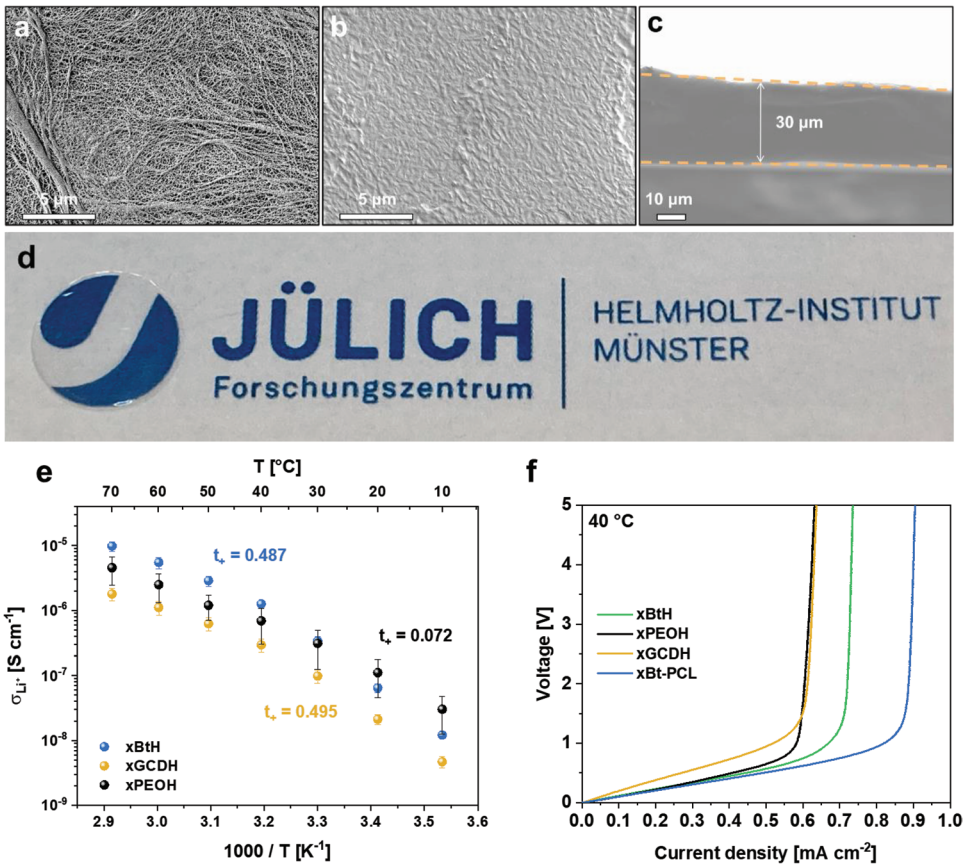

Figure 2. Scanning electron microscope (SEM) images of a) 5 µm PE separator (top view), b) the hybrid membrane xBtH (top view) and c) a cross-sectional view of the hybrid membrane. d) A photograph of transparent xBtH membrane (14 mm in diameter). e) lithium-ion conductivity (σ_{Li}) for three thin hybrid SPEs with their lithium-ion transference numbers ([C=O]:[Li] = 5:1 for PCL and [EO]:[Li] = 10:1 for PEO). Potentiostatic polarization experiments and impedance data are included in Figure S13 (Supporting Information). f) Galvanodynamic determination of the limiting current density at a sweep rate of 1 µA s^{-1} at 40 °C.

liquid component should be present within the materials. Due to the solid polymeric nature of PEO and PCL as well as comparable thermal stability, it is expected that they will likely perform similarly when subjected to cell safety tests. Further increase in energy density could theoretically be achieved with cathodes with even higher mass loadings (e.g., 20 mg cm^{-2} to achieve 570 Wh L^{-1}), but requires further optimization of the cathode infiltration and is currently under investigation.

2.2. Upscaling and Characterization of the Biopolymer Electrolytes

The synthesis of non-cross-linked GCD-PCL is straightforward comparable to the preparation of Bt-PCL. An organic catalyst (1,5,7-triazabicyclo[4.4.0]dec-5-ene, TBD) was utilized for ring-opening polymerization enabling an ambient reaction temperature. A minimum amount of solvent (20 mL) was used to dissolve the catalyst. A high reaction yield of 95 % can be achieved and the molecular weight of the hyper-branched polymer was determined by gel permeation chromatography (GPC), revealing a narrow dispersity (M_n = 7.6 × 10^4 g mol^{-1}, M_w = 9.2 × 10^4 g mol^{-1} and $Đ$ = 1.2, see Figure S3, Supporting Information). The polymer structure was defined based on ^{1}H and ^{13}C NMR data (see Figures S4,S5, Supporting Information). The grafting density of PCL side chains on the α-CD units is estimated as 82.6 %, i.e., 15 out of 18 available initiation sites (-OH units) are covalently attached to PCL chains. Both PCL-based polymer electrolytes are up-scalable in a 2 L reactor (IKA). In a first attempt, 130 g of GCD-PCL and 470 g of Bt-PCL were successfully produced with overall yields of 83 % and 94 %, respectively (Figure S6, Supporting Information). GPC analysis indicates a reproducible polymerization comparable to that of the lab-scale synthesis (Figure S7, Supporting Information).

The ionic conductivity of the hybrid membranes was compared to that of the pristine ones (Figure S10a, Supporting Information). Though the overall ionic conductivity of hybrid membranes is reduced due to non-conductive PE porous scaffold, the ionic conductance, which is reversely proportional to the thickness, is maintained and even increased as a result of shorter lithium-ion diffusion time and pathways (see Figure S10b, Supporting Information).[6b] The lithium-ion conductivity σ_{Li^+} and transference number of the hybrid membranes is shown in Figure 2e. While xBtH and xGCDH have similar cation transference numbers (t_+) around 0.49, xPEOH has a very low t_+ (0.072), resulting in smaller difference of σ_{Li^+}

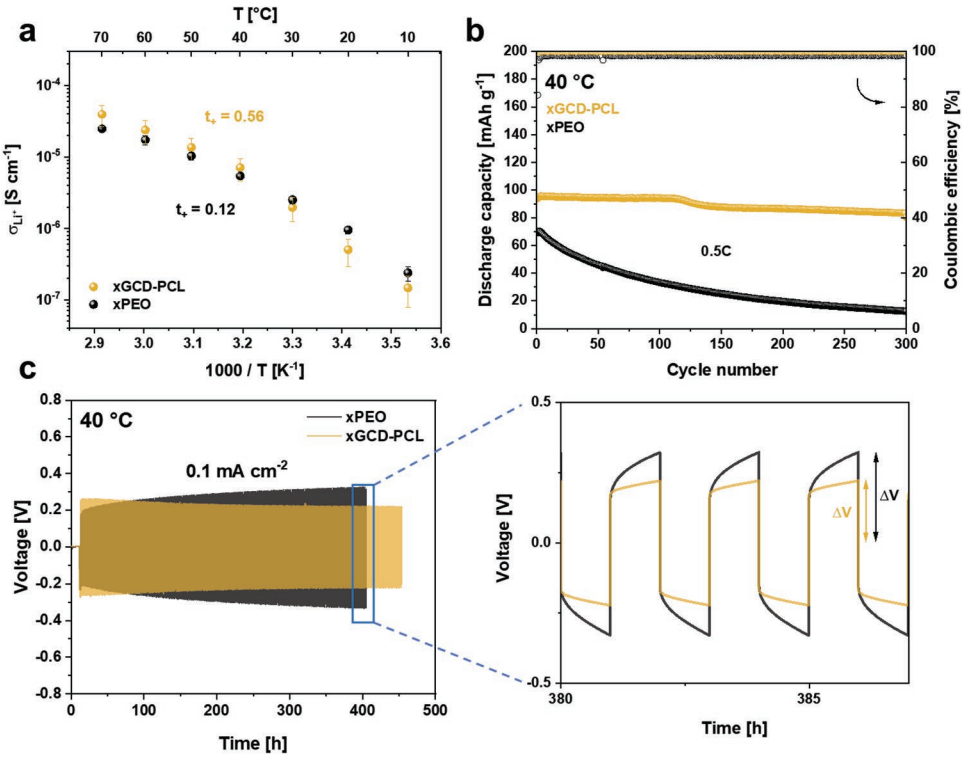

Figure 3. Electrochemical measurements for xGCD-PCL and xPEO. a) Lithium-ion conductivity (σ_{Li}) with their lithium-ion transference numbers ([C=O]:[Li] = 5:1 for PCL and [EO]:[Li] = 10:1 for PEO). Potentiostatic polarization experiments and impedance data are included in Figure S12 (Supporting Information). b) Long-term cycling of NMC622|SPE|Li cells at 0.5 C, 40 °C in 3.0–4.3 V (300 µm Li and 100 µm SPE; cathode mass loading: 2.5 mg cm^{-2}). Pre-cycles: 0.05 C × 2, 0.1 C × 3, 0.2 C × 3, 0.5 C × 3 and 1 C × 3. c) Long-term lithium plating/stripping experiment.

among the three types of solid polymer electrolytes (Figure 2e). The higher lithium-ion mobility of the PCL-based electrolytes is attributed to the weaker coordination between carbonyl moieties and Li^+ compared to ether-Li^+ interactions in PEO.[13]

In view of potential fast charge applications, the actual limiting current densities of the thin membranes were determined based on a galvano-dynamic sweep until a cut-off voltage is reached (Figure 2f). Both xPEOH and xGCDH achieved a limiting current density of 0.62 mA cm^{-2}, whereas xBtH reached 0.73 mA cm^{-2}. With a value of 0.89 mA cm^{-2}, the thick membrane (xBt-PCL) can withstand the largest current density, most likely due to the slightly better ion transport parameters of the pristine polymer membranes (i.e., higher ionic conductivity). Considering fast charging capability solely of the electrolyte materials, they could withstand a theoretical charging rate of 0.5 C at a specific capacity of 175 mAh g^{-1} at 6 mg cm^{-2} active mass loading (current density of 0.525 mA cm^{-2}). Practical limitations of both cathodes and anodes at higher current densities, however, require operation at lower charging rates such as 0.25 C at 40 °C.

The advantage of pure xGCD-PCL compared to xPEO is further demonstrated in **Figure 3**. The transference number of xGCD-PCL is higher compared to that of xPEO (0.56 and 0.12, respectively). The lower t_+ for xPEO not only leads to smaller overall lithium-ion conductivity (σ_{Li^+}) above 40 °C, but also manifests itself in unfavorable electrochemical performance during reversible Li plating/stripping experiments or long-term cycling as it may facilitate concentration polarization.[21] Notably, xGCD-PCL shows a much better cell cycling performance at 40 °C (cathode mass loading: 2.5 mg cm^{-2}) compared to xPEO (Figure 3b), affording a capacity retention of 87.3 % over 300 cycles, as well as lower overvoltage upon Li plating/stripping (Figure 3c). Also, the oxidative stability of polymer electrolytes also plays a critical role, especially upon cycling against high-voltage cathode materials (e.g., NMC622/811) or applying a constant voltage (CV) step during the charge process. PEO-type electrolytes are known for relatively lower oxidative stability up to cut-off voltages of 4.6 V, as determined in NMC622|SPE|Li cell set-up.[22] In contrast, the PCL-based polymers are oxidatively stable beyond 5 V (Figure S11, Supporting Information).

2.3. Boosting Cathode Capacity Through Oligomers

The synthetic route for making caprolactone oligomers (PCL400) are highlighted in Scheme S1 (Supporting Information). For the production of linear intermediate oligomer (PCL400OH), 1-propanol was used as initiator with enough solvent to dissolve TBD catalyst. Since the presence of terminal hydroxyl groups are regarded as "fatal" species for operation of high-voltage lithium batteries,[23] dimethyl carbonate (DMC) was utilized for dihydroxylation of PCL400OH.[24] The oligomer PCL400 affords a higher ionic conductivity (0.2 mS cm^{-1}) than the xBt-PCL polymer (0.02 mS cm^{-1}) due to chain dynamics, rendering it a suitable catholyte for enabling high mass loading

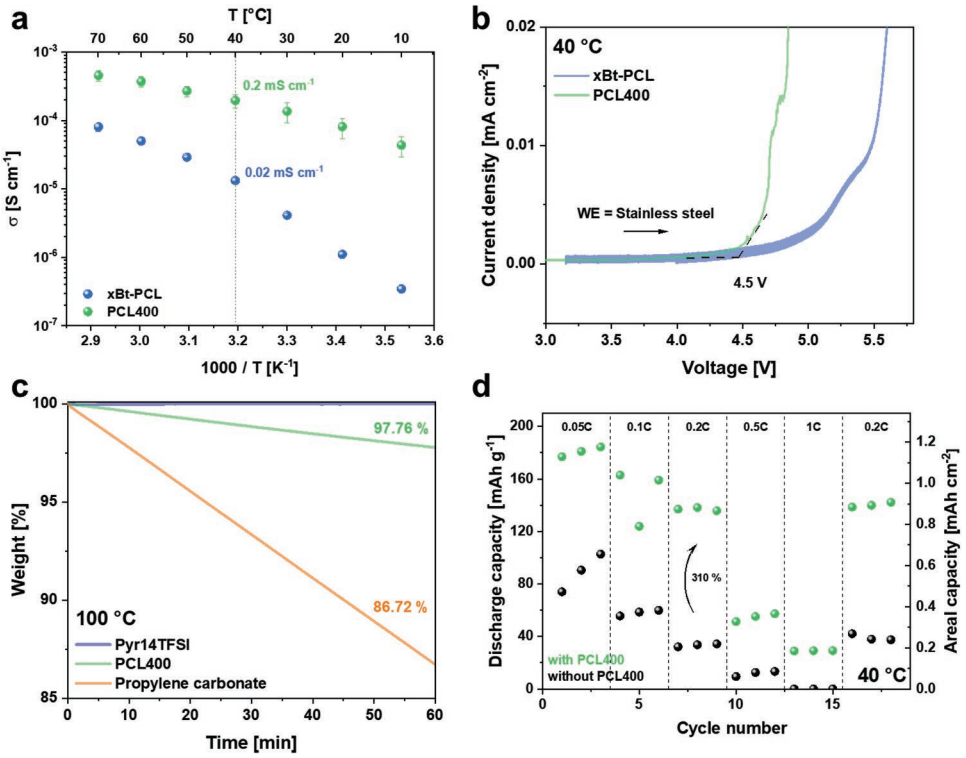

Figure 4. a) Overall ionic conductivity of xBt-PCL and PCL400 at [C=O]:[Li] ratio of 5:1, b) oxidative stability of PCL400 oligomer and xBt-PCL. c) Weight loss of various additives at 100 °C for 1 h (He flow of 25 mL min^{-1}). d) C-rate performance of NMC622|xBt-PCL|Li cells with/without PCL400 at 40 °C in the voltage range of 3–4.3 V (300 µm Li and 100 µm SPE; cathode mass loading: 6 mg cm^{-2}).

cathode applications (see **Figure 4**a; Figure S9, Supporting Information). Despite a slightly decreased electrochemical stability window compared to xBt-PCL (Figure 4b), the oligomer PCL400 is sufficiently robust to voltages of up to ca. 4.5 V.[25] Additionally, niobate-coated NMC622 was exploited as cathode material to mitigate potential side reactions between transition metal ions and the respective catholytes.[26]

Thermogravimetric analyses (TGA) were performed to verify the low volatility of PCL400, in comparison to other common additives/solvents applied in LMBs, including the non-volatile ionic liquid reference 1-butyl-1-methylpyrrolidinium bis(trifluoromethylsulfonyl)imide (Pyr14TFSI) (see Figure 4c). Notably, PCL400 experiences merely 2.24 % weight loss after 1 h of heating at 100 °C, compared to a loss of 13.28 % in case of propylene carbonate (PC). This indicates that oligomer-based additives with low vapor pressure could be safer options for LMBs while maintaining sufficiently high ionic conductivity. The rate capability of cells with higher cathode mass loading (6 mg cm^{-2}) demonstrates the beneficial effect of the catholyte, as shown in Figure 4d. At 40 °C, the NMC622|xBt-PCL|Li cells (SPE thickness: 100 µm) with PCL400 deliver significantly increased capacities compared to pristine cells, especially at rates of 0.2 C.

Galvanostatic intermittent titration technique (GITT) of NMC622|xBtH|Li cells was conducted to validate the anticipated benefits of PCL400 catholyte on the resulting discharge capacity. A series of current pulses of 0.1 C (84.6 µA) was applied to cells with and without catholyte for 10 min, followed by a relaxation period of 1 h until the cut-off voltages of either 4.3 V (charge) or 3.0 V (discharge) was reached (**Figure 5**a). Significant variations can be seen in the IR drop and the charge/discharge times between two samples, indicating smaller Ohmic and charge transfer resistances in case of cells with PCL400.[27] The effective chemical lithium-ion diffusion coefficients (D_{Li^+}) within the active material were determined based on Equation S4 (see Supporting Information and Figure 5b). Overall, D_{Li^+} of the cells with PCL400 are three times higher than those of the pristine cells during charge steps, and the difference is gradually increasing with the degree of lithiation within the discharge steps. Note that the apparent diffusion coefficient varies with the state of charge in a complex mode, not only depending on the degree of lithiation, but also on the changes of lattice parameters including phase transformations of the cathode active materials.[28]

2.4. Full Cell Prototypes

NMC622|SPE|Li cells were assembled in a "Generation II" set-up and cycled at 0.25 C at 60 °C (**Figure 6**a), as PEO-based cells are typically operated at temperatures of 60 °C or higher for better electrochemical performance.[29] xPEOH cells show an initial capacity of 124 mAh g^{-1} at 0.25 C, which is comparable to xGCDH cells (theoretical capacity: 175 mAh g^{-1}); however, it exhibited more rapid fading as consequence of faster oxidative degradation at higher temperatures. Cells with pristine xBt-PCL membranes (100 µm) were also included in contrast to xBtH cells. Unfavorable Coulombic efficiencies for the

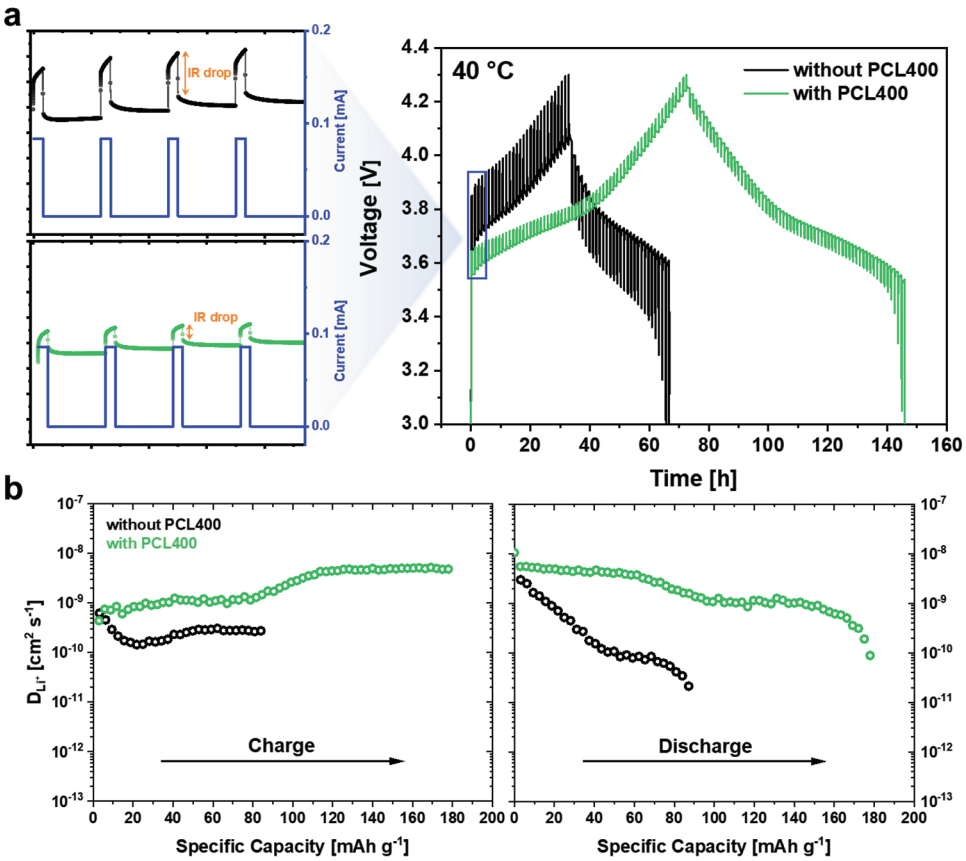

Figure 5. a) Galvanostatic intermittent titration curve versus time of NMC622 cathodes with/without caprolactone oligomer at 40 °C, with the imposed current (0.1 C, 10 min) and resulting voltage response in the first few charge steps. The relaxation period is 1 h. b) Derived lithium-ion diffusion coefficients as a function of specific capacity.

thicker 100 µm membrane were observed, most likely reflecting "voltage noise" due to Li dendrites-induced micro-short circuit.[7] The phenomenon happened not only at 60 °C, but even at 40 °C. A supporting matrix like the hybrid concept applied in SPE membranes is needed to ensure sufficient mechanical strength, especially at higher current densities. Notably, xBtH cells delivered a higher initial capacity of 185 mAh g^{-1} corresponding to areal capacities of ca. 1.16 mAh cm^{-2}, illustrating better wettability of xBt-PCL and oligomer catholytes. Although both xBtH and xGCDH are PCL-based materials, variations in discharge capacity were observed. The xGCDH shows reduced ionic conductivity upon introducing the PE scaffold; however, the caprolactone oligomer seems to be more compatible with xBtH electrolytes.

To go beyond PEO and its high operating temperatures, all cells were also tested at 40 °C (Figure 6b). This temperature is considered practical and acceptable for EVs fast-charging particularly when using solid-state electrolytes, according to Quantumscape's white paper.[30] xPEOH demonstrates a drastically decreased capacity as it is outside of its thermal operational window (60 to 80 °C). xGCDH cells have a much higher initial capacity (105 mAh g^{-1}) compared to xPEOH, which is also reflected in the lower overall internal resistance (Figure S14, Supporting Information). The overall polarization resistance of xPEOH cells (725 Ω cm^2) is larger compared to all other cells and the characteristic diffusive tail at lower frequencies is missing, indicating a poor charge transport within the cathode (see Figure S15, Supporting Information, for the resistance evolution before and after formation). The resistive contribution at medium frequencies (318 Hz or 0.5 ms, corresponding to charge transport at interfaces and interphases) is also largest for the xPEOH cell with roughly 215 Ω cm^2, as can be derived from the distribution of relaxation times (DRT) analysis (Figure S14, Supporting Information). Note that the area of DRT intensity is proportional to the real resistance (i.e., the radius of the "semicircle" in the Nyquist plot). EIS data and DRT analysis of symmetric Li||Li cells (Figure S16, Supporting Information) reveal comparable interfacial resistances of xPEOH (683 Ω cm^2) and xBtH (757 Ω cm^2) at medium frequency ranges, rendering the cathode interface as a major factor of the large interfacial resistances in case of xPEOH-based cells.

The xBtH cells delivered initial capacities of 167 mAh g^{-1}, corresponding to areal capacities of ca. 0.99 mAh cm^{-2}. This comparatively high initial capacity correlates with EIS and DRT data, as the overall resistance of 549 Ω cm^2 is lowest for xBtH cell. Interestingly, the impedance response of cells operated with thin xBtH and thick xBT-PCL membranes is rather similar, with an exception of lower bulk resistance (due to reduced thickness) and lower impedance for xBtH at low frequencies (high time constants >10^{-2} s in Figure S14, Supporting Information). The

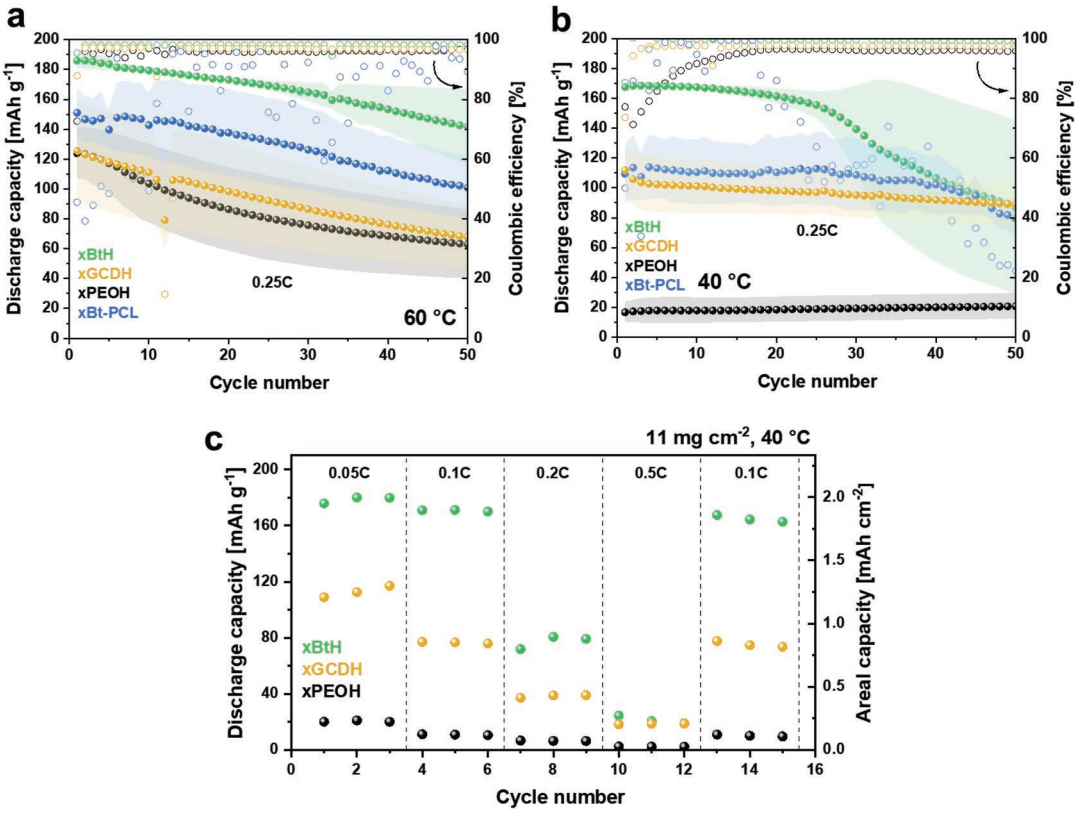

Figure 6. NMC622|SPE|Li cells in generation II set-up (except for xBt-PCL: 100 µm thick) with PCL400 cycling at 0.25 C, a) 60 °C and b) 40 °C in 3.0–4.3 V (inner coin cell pressure: 0.43 MPa); (cathode mass loading: 6 mg cm^{-2}). Formation cycles: 0.05 C × 2, 0.1 C × 2, and 0.05 C × 2. c) C-rate performance of NMC622|SPE|Li cells with PCL400 at 40 °C in the voltage range of 3–4.3 V (cathode mass loading: 11 mg cm^{-2}).

caprolactone oligomer is considered stable against the NMC622 cathode, due to its high oxidative stability (4.5 V) as well as the $LiNbO_3$ coating on the surface of NMC particles. No self-polymerization of oligomer was observed during charge and discharge. This was reflected by xGCDH cells and their constant $R_{diff/int}$ (high time constants >10^{-2} s) before and after formation, as well as retentive discharge capacity over 50 cycles. The specific capacities of xGCDH and xBtH cells at 40 °C are only slightly smaller than that at 60 °C, indicating a relative independence to temperature changes for both PCL-based electrolytes. Moreover, xBtH electrolytes are able to cycle against NMC811 at cathode mass loadings of 6 mg cm^{-2}, yielding specific capacities of up to 181 mAh g^{-1} at 0.1 C upon formation (practical maximum capacity: 200 mAh g^{-1}), while xGCDH and xPEOH-based cells are unable to afford reasonable capacities in case of identical cell set-ups (Figure S17, Supporting Information). This indicates that further efforts are required to tune the compatibility among polymer electrolyte, oligomer catholyte and scaffold matrix to maximize the achievable cell capacities while reducing internal resistances. NMC622 with mass loading of 11 mg cm^{-2} was applied to further evidence the potential of the proposed hybrid cell concept (Figure 6c), where xBtH cells indeed delivered highly appreciable specific capacities of 179 and 170 mAh g^{-1}, respectively, at reasonable rates 0.05 or 0.1 C. Compared to commercialized PEO-type systems at 60 °C, polyester/oligomer-based hybrid cell set-ups exhibit larger capacities at 40 °C, as well as enhanced projected energy density of 356 Wh L^{-1}, superior to other reported cell systems (cf. Scheme 1b; Table S2, Supporting Information), clearly demonstrating the application potential of the proposed polymer-based hybrid cell concept, in principle going beyond generation 4 (IT3-E) models of Bolloré-based lithium metal polymer technology.

2.5. Limitations and Remaining Challenges

The observed capacity fading in case of xBtH cells remains a challenge. A possible explanation might be partial oligomer diffusion through the membrane to the lithium metal surface, where SEI dissolution and oligomer reduction are conceivable (Figure S18, Supporting Information). Considering the wettability or swelling of the applied polymer membranes, most of the oligomer migrated through xBtH, reaching the other side of the membrane, but almost no migration was determined for xPEOH, and only minor fractions in case of xGCDH membranes (Figure S19, Supporting Information). Meanwhile, we observed better swelling behavior of xGCD-PCL upon exposure to oligomers, though the oligomers eventually penetrate the hybrid membranes, so that diffusion to the Li anode may occur. Future efforts will be devoted to achieve pronounced barrier effects of the polymer membrane in contact with the cathode, as well as novel infiltration techniques. When cycling at ambient temperature, the migration of the oligomer is likely slower, eventually accountable for comparably good electrochemical performance

of xBtH at 20 °C, with a capacity retention of 98.5% after 150 cycles (Figure S20, Supporting Information) at 0.1 C and a mass loading of 2.5 mg cm^{-2}. The niobate-coated NMC622 is unlikely to degrade the oligomer catholyte as it has been shown to keep other electrolytes such as propylene carbonate intact.[26b] Potential degradation may occur between short-chain oligomers and lithium metal anode, where small amounts of moisture in the electrolyte membrane (122 ppm) and within the oligomer (ca. 36 ppm) may be carried to the lithium metal surface, leading to formation of lithium hydroxide (LiOH). The strong base then reacted with present ester units to produce alcohols, which may trigger a following Claisen condensation.[31] Unraveling the possible degradation mechanisms that result in the capacity fading and suitable counter strategies will be explored in future work.

3. Conclusion

In this contribution, a promising hybrid cell concept for polymer-based solid-state batteries is introduced in an effort to approach faster charge conditions and reduce the total thickness of cell components and resulting cell, in this way boosting the available (projected) cell energy densities. Scaffold-supported polymer electrolytes allow for solvent-free manufacture of ultra-thin membranes (thickness: 30 µm) thereby reducing overall internal and charge transfer resistances. Going beyond PEO, tailor-made poly-caprolactone-based electrolytes (xGCD-PCL and xBt-PCL) are exploited, along with fluid caprolactone oligomers functioning as catholyte additives and improving lithium-ion transfer within the composite cathodes. The production of PCL-based materials is rather straightforward and readily up-scalable (batch sizes of >100 g) as demonstrated for both Bt-PCL and GCD-PCL. Short-chain oligomers PCL400 exhibit significantly higher ionic conductivity (0.2 mS cm^{-1} at 40°C), enabling NMC622||Li cells with cathode mass loadings of up to 11 mg cm^{-2} and appreciable discharge capacities of 170 mAh g^{-1} (11 mg cm^{-2}) and 160 mAh g^{-1} (6 mg cm^{-2}) at reasonable rates of 0.1 C and 0.25 C, respectively, (considering Batteries Europe 2030 goals of 0.3 C for light duty battery electric vehicles (BEVs)).[32] Notably, the resulting overall single cell layer thickness below 150 µm (including the thickness of the corresponding polymer-based electrolyte, Li metal anode, cathode and current collector) affords a projected superior energy density of 356 Wh L^{-1}, even higher than in case of Bolloré-type PEO-based cells, also superior to other reported cell systems. In addition, low volatility of the oligomers renders them potentially safer additives for realizing higher energy density lithium metal batteries compared to common liquid electrolyte additives, even more affordable than most ionic liquids. In summary, flowable oligomers and thin scaffold supported polymer electrolytes are introduced to achieve high energy density applications of polymer-based hybrid cells.

Supporting Information

Supporting Information is available from the Wiley Online Library or from the author.

Acknowledgements

The authors gratefully acknowledge generous support by the German Federal Ministry of Education and Research (BMBF) within the grants "FB2-POLY" (13XP0429A), "FB2-Hybrid" (13XP0428A), "LiSI" (13XP0224A) and "LISI-2" (13XP0509A).

Open access funding enabled and organized by Projekt DEAL.

Conflict of Interest

The authors declare no conflict of interest.

Data Availability Statement

The data that support the findings of this study are available from the corresponding author upon reasonable request.

Keywords

flowable oligomers, lithium metal batteries, polycaprolactones, polymer electrolytes, thin hybrid electrolytes

Received: February 1, 2023
Revised: March 15, 2023
Published online: April 25, 2023

[1] a) F. Cherubini, T. Gasser, R. M. Bright, P. Ciais, A. H. Strømman, *Nat. Clim. Change* **2014**, *4*, 983; b) L. E. Erickson, *Environ. Prog. Sustainable Energy* **2017**, *36*, 982.

[2] a) T. Dietz, K. A. Frank, C. T. Whitley, J. Kelly, R. Kelly, *Proc. Natl. Acad. Sci. USA* **2015**, *112*, 8254; b) J. B. Dunn, L. Gaines, J. C. Kelly, C. James, K. G. Gallagher, *Energy Environ. Sci.* **2015**, *8*, 158.

[3] a) J. Li, Y. Cai, H. Wu, Z. Yu, X. Yan, Q. Zhang, T. Z. Gao, K. Liu, X. Jia, Z. Bao, *Adv. Energy Mater.* **2021**, *11*, 2003239; b) D. Puthusseri, M. Wahid, S. Ogale, *Energy Fuels* **2021**, *35*, 9187.

[4] a) D. Lisbona, T. Snee, *Process Saf. Environ. Prot.* **2011**, *89*, 434; b) E. P. Roth, C. J. Orendorff, *Electrochem Soc Interface* **2012**, *21*, 45; c) L. M. Rodriguez-Martinez, N. Omar, *Emerging nanotechnologies in rechargeable energy storage systems*, William Andrew, Norwich, New-York, **2017**; d) J. R. Nair, L. Imholt, G. Brunklaus, M. Winter, *Electrochem Soc Interface* **2019**, *28*, 55.

[5] a) X. Judez, G. G. Eshetu, C. Li, L. M. Rodriguez-Martinez, H. Zhang, M. Armand, *Joule* **2018**, *2*, 2208; b) Q. Zhou, J. Ma, S. Dong, X. Li, G. Cui, *Adv. Mater.* **2019**, *31*, 1902029.

[6] a) R. Jung, P. Strobl, F. Maglia, C. Stinner, H. A. Gasteiger, *J. Electrochem. Soc.* **2018**, *165*, A2869; b) J. Wu, Z. Rao, Z. Cheng, L. Yuan, Z. Li, Y. Huang, *Adv. Energy Mater.* **2019**, *9*, 1902767.

[7] Y.-H. Chen, Y.-C. Hsieh, K. L. Liu, L. Wichmann, J. H. Thienenkamp, A. Choudhary, D. Bedrov, M. Winter, G. Brunklaus, *Macromol. Rapid Commun.* **2022**, *43*, 2200335.

[8] a) K.-m. Shin, T. Dong, Y. He, Y. Taguchi, A. Oishi, H. Nishida, Y. Inoue, *Macromol. Biosci.* **2004**, *4*, 1075; b) K.-M. Shin, T. Dong, K. Yazawa, S.-S. Im, Y. Inoue, *J. Polym. Sci., Part B: Polym. Phys.* **2008**, *46*, 879; c) L. Imholt, T. S. Dörr, P. Zhang, L. Ibing, I. Cekic-Laskovic, M. Winter, G. Brunklaus, *J. Power Sources* **2019**, *409*, 148; d) L. Imholt, D. Dong, D. Bedrov, I. Cekic-Laskovic, M. Winter, G. Brunklaus, *ACS Macro Lett.* **2018**, *7*, 881.

[9] a) A. Celebioglu, T. Uyar, *J. Agric. Food Chem.* **2019**, *67*, 13093; b) T. Loftsson, P. Jarho, M. Másson, T. Järvinen, *Expert Opin. Drug*

Delivery **2005**, *2*, 335; c) S. J. Kim, G. B. Park, C. B. Kang, S. D. Park, M. Y. Jung, J. O. Kim, Y. L. Ha, *J. Agric. Food Chem.* **2000**, *48*, 3922.

[10] a) J. Herzberger, K. Niederer, H. Pohlit, J. Seiwert, M. Worm, F. R. Wurm, H. Frey, *Chem. Rev.* **2016**, *116*, 2170; b) D. Krause, M. Grünebaum, H.-D. Wiemhöfer, M. Winter, *Patent WO 2022/008615 A1* **2022**.

[11] a) M. M. Benmassaoud, C. Kohama, T. W. B. Kim, J. A. Kadlowec, B. Foltiny, T. Mercurio, S. I. Ranganathan, *Biomed. Microdevices* **2019**, *21*, 51; b) S. M. Espinoza, H. I. Patil, E. San Martin Martinez, R. Casañas Pimentel, P. P. Ige, *Int. J. Polym. Mater. Polym. Biomater.* **2020**, *69*, 85; c) C. P. Fonseca, D. S. Rosa, F. Gaboardi, S. Neves, *J. Power Sources* **2006**, *155*, 381.

[12] H. Xu, J. Xie, Z. Liu, J. Wang, Y. Deng, *MRS Energy Sustain* **2020**, *7*, E2.

[13] M. P. Rosenwinkel, R. Andersson, J. Mindemark, M. Schönhoff, *J. Phys. Chem. C* **2020**, *124*, 23588.

[14] a) J. Mindemark, B. Sun, E. Törmä, D. Brandell, *J. Power Sources* **2015**, *298*, 166; b) C. Sångeland, R. Younesi, J. Mindemark, D. Brandell, *Energy Storage Mater.* **2019**, *19*, 31; c) B. Zhang, Y. Liu, X. Pan, J. Liu, K. Doyle-Davis, L. Sun, J. Liu, X. Jiao, J. Jie, H. Xie, *Nano Energy* **2020**, *72*, 104690; d) D. Zhang, L. Zhang, K. Yang, H. Wang, C. Yu, D. Xu, B. Xu, L.-M. Wang, *ACS Appl. Mater. Interfaces* **2017**, *9*, 36886; e) B. Zhang, Y. Liu, J. Liu, L. Sun, L. Cong, F. Fu, A. Mauger, C. M. Julien, H. Xie, X. Pan, *J Energy Chem* **2021**, *52*, 318; f) W. Ye, M. Zaheer, L. Li, J. Wang, H. Xu, C. Wang, Y. Deng, *J. Electrochem. Soc.* **2020**, *167*, 110532; g) T. K. Lee, R. Andersson, N. A. Dzulkurnain, G. Hernández, J. Mindemark, D. Brandell, *Batteries Supercaps* **2021**, *4*, 653; h) P.-M. Jalbert, B. Commarieu, J.-C. Daigle, J. P. Claverie, K. Zaghib, *J. Electrochem. Soc.* **2020**, *167*, 080527.

[15] a) K. Inoue, *Prog. Polym. Sci.* **2000**, *25*, 453; b) R. L. Kerr, S. A. Miller, R. K. Shoemaker, B. J. Elliott, D. L. Gin, *J. Am. Chem. Soc.* **2009**, *131*, 15972; c) T. F. Miller Iii, Z.-G. Wang, G. W. Coates, N. P. Balsara, *Acc. Chem. Res.* **2017**, *50*, 590; d) T. Niitani, M. Amaike, H. Nakano, K. Dokko, K. Kanamura, *J. Electrochem. Soc.* **2009**, *156*, A577; e) H. Wakayama, H. Yonekura, Y. Kawai, *Chem. Mater.* **2016**, *28*, 4453; f) M. A. Webb, Y. Jung, D. M. Pesko, B. M. Savoie, U. Yamamoto, G. W. Coates, N. P. Balsara, Z.-G. Wang, T. F. Miller Iii, *ACS Cent. Sci.* **2015**, *1*, 198.

[16] S. Ma, M. Jiang, P. Tao, C. Song, J. Wu, J. Wang, T. Deng, W. Shang, *Prog. Nat. Sci.: Mater. Int.* **2018**, *28*, 653.

[17] a) H. Xu, W. Ye, Q. Wang, B. Han, J. Wang, C. Wang, Y. Deng, *J. Mater. Chem. A* **2021**, *9*, 9826; b) Z. Wang, L. Shen, S. Deng, P. Cui, X. Yao, *Adv. Mater.* **2021**, *33*, 2100353; c) Y. Ma, J. Wan, Y. Yang, Y. Ye, X. Xiao, D. T. Boyle, W. Burke, Z. Huang, H. Chen, Y. Cui, Z. Yu, S. T. Oyakhire, Y. Cui, *Adv. Energy Mater.* **2022**, *12*, 2103720; d) E. Fedeli, O. Garcia-Calvo, A. Gutiérrez-Pardo, T. Thieu, I. Combarro, R. Paris, J. Nicolas, H.-J. Grande, I. Urdampilleta, A. Kvasha, *Solid State Ionics* **2023**, *392*, 116148.

[18] I. Osada, H. de Vries, B. Scrosati, S. Passerini, *Angew. Chem.* **2016**, *55*, 500.

[19] Q. Zhao, X. Liu, S. Stalin, K. Khan, L. A. Archer, *Nat. Energy* **2019**, *4*, 365.

[20] a) Y. S. Wu, Q.-T. Pham, C.-C. Yang, C.-S. Chern, L. M. Babulal, M. Seenivasan, J. Jeyakumar, T. H. Mengesha, T. Placke, G. Brunklaus, M. Winter, B. J. Hwang, *ACS Sustainable Chem. Eng.* **2022**, *10*, 7394; b) M. Seenivasan, J. Jeyakumar, Y.-S. Wu, Q.-T. Pham, C.-S. Chern, B.-J. Hwang, C.-C. Yang, *Composites, Part B* **2022**, *242*, 110083.

[21] M. Doyle, T. F. Fuller, J. Newman, *Electrochim. Acta* **1994**, *39*, 2073.

[22] G. Homann, L. Stolz, M. Winter, J. Kasnatscheew, *iScience* **2020**, *23*, 101225.

[23] X. Yang, M. Jiang, X. Gao, D. Bao, Q. Sun, N. Holmes, H. Duan, S. Mukherjee, K. Adair, C. Zhao, J. Liang, W. Li, J. Li, Y. Liu, H. Huang, L. Zhang, S. Lu, Q. Lu, R. Li, C. V. Singh, X. Sun, *Energy Environ. Sci.* **2020**, *13*, 1318.

[24] W.-C. Shieh, S. Dell, O. Repič, *J. Org. Chem.* **2002**, *67*, 2188.

[25] K. Khan, Z. Tu, Q. Zhao, C. Zhao, L. A. Archer, *Chem. Mater.* **2019**, *31*, 8466.

[26] a) A. Y. Kim, F. Strauss, T. Bartsch, J. H. Teo, T. Hatsukade, A. Mazilkin, J. Janek, P. Hartmann, T. Brezesinski, *Chem. Mater.* **2019**, *31*, 9664; b) M.-H. Chiou, K. Borzutzki, J. H. Thienenkamp, M. Mohrhardt, K.-L. Liu, V. Mereacre, J. R. Binder, H. Ehrenberg, M. Winter, G. Brunklaus, *J. Power Sources* **2022**, *538*, 231528.

[27] A. Nickol, T. Schied, C. Heubner, M. Schneider, A. Michaelis, M. Bobeth, G. Cuniberti, *J. Electrochem. Soc.* **2020**, *167*, 090546.

[28] a) Y. Zhu, C. Wang, *J. Phys. Chem. C* **2010**, *114*, 2830; b) A. Van der Ven, J. Bhattacharya, A. A. Belak, *Acc. Chem. Res.* **2013**, *46*, 1216.

[29] a) J. Mindemark, M. J. Lacey, T. Bowden, D. Brandell, *Prog. Polym. Sci.* **2018**, *81*, 114; b) A. Varzi, K. Thanner, R. Scipioni, D. Di Lecce, J. Hassoun, S. Dörfler, H. Altheus, S. Kaskel, C. Prehal, S. A. Freunberger, *J. Power Sources* **2020**, *480*, 228803.

[30] QuantumScape White Paper, A deep dive into QuantumScape's fast charging performance, *QuantumScape* **2022**.

[31] M. Grünebaum, A. Buchheit, C. Lürenbaum, M. Winter, H.-D. Wiemhöfer, *J. Phys. Chem. C* **2019**, *123*, 7033.

[32] E. Commission, Batteries Europe, *Roadmap – Application and Integration: Mobile* **2021**.